ARCHIVES

of

FOUNDRY ENGINEERING

Effect of Heat Treatment T6 on Selected Properties and Structure of AlSi5Cu2Mg Alloy with Addition of Mo, Zr, and Sr

M. Sýkorová [a], * (iD) **, D. Bolibruchová** [a] (iD) **, M. Brůna** [a] (iD) **, K. Hradečný** [b] (iD)

[a] University of Zilina, Slovak Republik

[b] VSB - Technical University of Ostrava: Ostrava, Czech Republik

* Corresponding author: E-mail address: martina.sykorova@fstroj.uniza.sk

Abstract

The hypoeutectic aluminum alloy AlSi5Cu2Mg is used for the production of high-strength automotive components such as cylinder head castings. AlSi5Cu2Mg alloy is characterized by a specific chemical composition (low permitted Si and Ti content) determined by the supplier. Due to the low permitted Ti content it is impossible to refine the grain structure of this aluminum alloy using standard grain refiners based on Al-Ti-B. Al-Si-Cu-Mg alloys are thermal stable up to the temperature 200 °C, due to the presence of strengthening precipitates. Due to the downsizing, the operating temperature exceeds the temperature of 200 °C, which leads to a decrease in the mechanical and physical properties of Al-Si-Cu-Mg alloys. The aim of this study is to analyse influence the alloying elements and heat treatment on the selected properties of AlSi5Cu2Mg alloys that are crucial for cylinder head castings. The paper focuces on the evaluation of the influence of selected alloying elements Sr, Zr and Mo on mechanical and physical properties. The present work also analysis the effect of heat treatment T6 on selected properties and structure of AlSi5Cu2Mg alloy modified by Sr, Zr or Mo. Sr, Zr and Mo were added into the AlSi5Cu2Mg alloy in the form of master alloys AlMo10, AlSr10 or AlZr20. According to the findings, the incorporation of the chosen alloying elements did not result in a substantial improvement in the mechanical and physical characteristics of AlSi5Cu2Mg alloy, which would be critical for its practical application. Physical and mechanical properties noted positive increase due to the effect of thermal processing T6.

Keywords: Heat treatment, Molybdenum, Zirconium, Strontium

1. Introduction

In recent years, internal combustion engines have undergone significant changes due to the strict emission standards [1]. Downsizing is the new trend in automotive industry which focuses on reducing the number of cylinders and reducing engine displacement while maintaining or increasing engine power [2]. Downsizing leads to the elimination of emission production. Li states that the weight of each car decreased by 10%, fuel consumption decreased by 8%, and emissions by 4% [3]. On the other side, downsizing leads to an increase in the temperatures of the combustion process and thus the operating temperatures of high-stress automotive components based on Al-Si-Cu-Mg [4].

Al-Si-Cu-Mg alloys have been widely used in the automobile industry due to their high strength-to-low weight ratio, excellent castability, high resistance to corrosion and favourable mechanical and physical characteristics [5]. Al-Si-Cu-Mg are

characterized by limited thermal stability (200 °C), which is limited by the elements Cu and Mg. Cu and Mg create Al_2Cu and Mg_2Si strengthening precipitates as a result of heat treatment [6,7]. Exceeding the temperature of 200 °C leads to a decrease in mechanical and physical properties due to the gradual thickening and dissolution of Al_2Cu and Mg_2Si strengthening precipitates [7]. Therefore, it is necessary to focus on the development of new thermally stable Al-Si-Cu-Mg alloys, which would have an optimal combination of mechanical and physical properties. The physical and mechanical properties of Al-Si-Cu-Mg alloys can be influenced by the use of heat treatment. Another possibility to effectively increase the physical and mechanical properties of Al-Si-Cu-Mg alloys is the use of alloying elements. [7-8]

Molybdenum finds significant application in the field of increasing the thermal stability of aluminum alloys based on Al-Si [9]. Mo introduced into the aluminum alloy melt in the form of master alloys (AlMo10, AlMo20, etc.) tends to form thermally stable dispersoids with a high concentration of Mo [10]. The presence of thermally stable Mo-based dispersoids leads to an increase in the thermal stability of aluminum alloys above 300 °C [9]. Mo acts as a corrector of Fe-based intermetallic phases and has a beneficial effect on the resulting mechanical properties and corrosion resistance of Al-Si-Cu-Mg alloys [9].

Zirconium is included in the group of transition metals and, like molybdenum, has a favourable effect on the resulting thermal stability of aluminum alloys [11]. Zr is mostly segregated in the form of intermetallic phases AlSiZr and Al_3Zr [12]. It is the Al_3Zr intermetallic phases that have high thermal stability and resistance to dissolution. Zr has a specific grain refinement effect on Al-Si-Cu-Mg alloys [13]. The effectiveness of this phenomenon is significantly influenced by the presence of elements Li and Zn, which suppress the crystallization of Al_3Zr intermetallic phases [14].

Strontium has a significant modifying effect on eutectic Si in hypoeutectic and eutectic Al-Si alloys. The modifying effect of Sr increases with increasing melt temperature and simultaneously increasing the dissolution rate of the Sr-based master alloy [15]. Adding trace levels of Sr has been known to change the morphology of Si from coarse plate to fine fibrous structure thus improving mechanical properties [16,17]. Literature survey has shown that the standard Sr addition to Al-Si alloys ranges from 0.015 - 0.025 wt.% Sr [18]. Pre-modification of the Al-Si-based alloy results in the crystallization of AlSrSi-based coarse and brittle particles, which leads to a decrease in mechanical properties [16].

The paper is aimed at investigating the influence of heat treatment T6 and the presence of alloying elements Mo, Sr and Zr on the resulting mechanical and physical properties and structure of the hypoeutectic aluminum alloy AlSi5Cu2Mg. AlSi5Cu2Mg alloy is specified by the manufacturer with a low permitted Ti content (0.03 wt. % max) and low Si content. The AlSi5Cu2Mg alloy is supplied to us by a foundry company that produces high-stress castings for the automotive industry such as cylinder heads. Ductility is a key feature that significantly affects the functionality of cylinder heads. For specific castings such as cylinder heads, achieving the minimum ductility value defined by designers can be a significant problem. Due to the specific chemical composition of the given alloy, the suppliers wanted to analyze the mechanical properties (especially ductility) and

physical properties of the given alloy alloyed with selected elements in excess addition after the specified T6 heat treatment. Excess additions of Mo and Sr, that extends well beyond the commercial practice and excess addition of Ti that exceeds manufacturer´s recommendations were tested in this work to identify all the potential effects of selected elements. The paper expands the knowledge about the AlSi5Cu2Mg alloy.

2. Materials and Methods

For an experimental work was chosen hypoeutectic aluminum AlSi5Cu2Mg alloy. AlSi5Cu2Mg alloy was marked like a reference alloy. Chemical composition of reference alloy is found in Table 1.

Table 1
Chemical composition of AlSi5Cu2Mg alloy – reference alloy [wt.%]

Si	Mg	Cu	Sr
5.412	0.292	1.859	0.008
Mo	**Ti**	**Mn/Fe**	**Al**
0.006	0.011	0.092	Bal.

The hypoeutectic aluminum alloy AlSi5Cu2Mg was melted in an electric resistance furnace. Experimental alloys were obtained by adding 0.15 wt.% Mo, 0.20 wt.% Zr or 0.12 wt.% Sr in the form of master alloys (AlMo10, AlZr20, and AlSr10) into the melt at a temperature of 770 °C ± 5 °C [19]. The element concentrations were chosen based on the recommendation of supplier, that focuses on the development of AlSi5Cu2Mg alloy. The experimental alloys were marked depending on the used element R-Mo, R-Zr and R-Sr. The chemical composition of the experimental alloys is shown in Table 2. [19]

Table 2
Chemical composition of experimental alloys [wt.%]

	R-Mo	R-Zr	R-Sr
Si	5.742	5.432	5.762
Fe	0.123	0.133	0.113
Cu	1.991	1.889	1.893
Sr	0.007	0.009	**0.112**
Zr	0.0006	**0.198**	0.0006
Mo	**0.119**	0.0007	0.0006
Ti	0.011	0.011	0.011
Al	Bal.	Bal.	Bal.

In the metallurgical process of melt preparation, the experimental alloys were not intentionally degassed. The samples were prepared by the technology of gravity casting into a metal mold (Fig. 1). The casting temperature was 740 °C ± 5 °C and the temperature of the metal mold was maintained in the temperature range of 180 °C - 200 °C [19]. A set of 10 samples was made for each experimental variant. Half of the samples were used to evaluate selected properties in the as-cast state, and the other half of the experimental samples were subjected to heat treatment by

precipitation hardening T6. The T6 thermal regime consisted of 3 steps:

- solution treatment at 520 °C ± 5 °C for 5.5 hours,
- quenching into hot water (70 °C ± 5 °C),
- artificial aging at 240 °C ± 5 °C for 5 hours.

A static tensile test was used to evaluate the experimental alloys' mechanical characteristics. The tensile test was carried out using an Inspekt desk 50 kN universal tearing device in accordance with EN ISO 6892-1 standards. The elongation value was determined from the tensile test working diagram based on an extensometer and subsequently recalculated against the evaluated length. The performance of the tensile test was made according to the relevant standard EN ISO 6892-1. The test specimens were chosen to be non-proportional. Therefore, dimensions of specimens were determined following the recommendations set out in the standard EN ISO 6892-1. For every experimental alloy, a set of five test circular rods with an 8 mm shank diameter were created. The scheme of the tensile test bar is shown in Fig. 1. The mechanical properties of the experimental samples were evaluated in the cast state and in the state after T6 heat treatment.
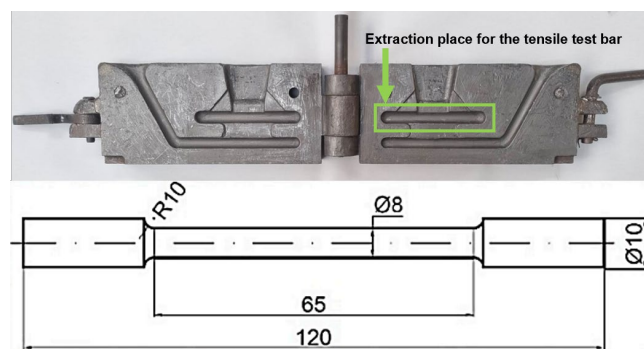
Fig. 1. Metal mold and scheme of tensile test bar

The hardness was determined by the Brinell hardness test (STN EN ISO 6506-1). The measurements were carried out with a Brinell Innovatest Nexus 3000 hardness tester according to HBW 5/250/10 (indentation body – 5 mm diameter carbide ball/load size 250 kp/load time 10 s). Five hardness measurements were performed on each experimental variant. Samples for hardness evaluation were taken from the tensile test bar. The hardness of the experimental alloys was evaluated in a transverse cross-section, and the samples were taken directly from the head of the tensile test bar.

Determination of the thermal conductivity (λ) of the experimental alloys was based on the evaluation of the electrical conductivity (σ) of the experimental alloys under examination using the Sigma Check 2 measuring device. Test samples with a diameter of 40 mm and a thickness of 9 mm were cast to evaluate the physical properties. The surfaces to be evaluated for physical properties were thoroughly cleaned and degreased before the measurement. The physical properties measurements were made at laboratory temperature in the range of 20 to 25 °C. The thermal conductivity (λ) was subsequently calculated from the electrical conductivity values by substituting into the empirical equation (1):

$$\lambda = 4.29 \cdot \sigma - 13.321 \ [W.m^{-1}.K^{-1}] \tag{1}$$

The microstructure of the experimental alloys was evaluated with a Neophot 32 optical microscope and TESCAN LMU II-line electron microscope with a BRUKER EDX analyser. The microstructural evaluation was performed on samples with the optimal combination of mechanical properties. The preparation of the experimental samples consisted of manual wet grinding, and polishing on polishing wheels impregnated with diamond paste and soaked with alcohol, followed by polishing with the automatic polishing device Struers Laboforce-3. The experimental samples intended for microstructural evaluation were etched with H_2SO_4.

3. Research Results and Discussions

3.1. Mechanical properties

The mechanical properties of the reference alloy, R-Mo, R-Sr and R-Zr in the as-cast state are processed in Fig. 2. The resulting mechanical properties represent average values from 5 measurements. The R-Mo alloy showed the best mechanical properties from the monitored set of experimental alloys. The ductility of the experimental alloy with Mo addition increased by 26 % compared to the reference alloy. The R-Sr alloy did not show significant changes in mechanical properties compared to the reference alloy. The hardness of the R-Sr alloy increased by 5 % compared to the reference alloy. The addition of Zr to the reference alloy caused a negative decrease in UTS and YS by 11 %, and 5 %, respectively, compared to the reference alloy. The decrease in mechanical properties of R-Zr could be caused by the morphology of the Zr-based intermetallic phases, which tend to precipitate in the form of single needles or clusters of two needles with slightly split ends, which act as stress concentrators. The R-Zr and R-Sr alloys showed the same ductility values as the reference alloy.
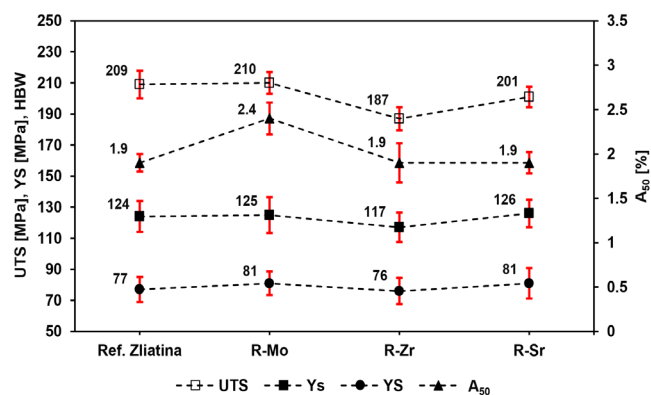
Fig. 2. Mechanical properties of experimental alloys in as-cast state [19]

The values of the mechanical properties of the experimental alloys after T6 heat treatment are processed into the graphical dependence at Fig. 3. The highest values of UTS and YS were achieved by the alloy with Sr addition. The UTS of the R-Sr alloy

increased by 5 % and the YS increased by 6 % compared to the reference alloy after T6. Due to the effect of T6, the R-Sr ductility showed the same values as reference alloy. On the contrary, the most significant increase in ductility and hardness was recorded by the experimental alloy with the addition of Mo. Compared to the reference alloy, ductility increased by 24 % and hardness by 15 %. The R-Mo alloy did not show a significant increase in YS compared to the reference alloy. The alloy with the addition of Zr did not show a significant increase in mechanical properties compared to the reference alloy.
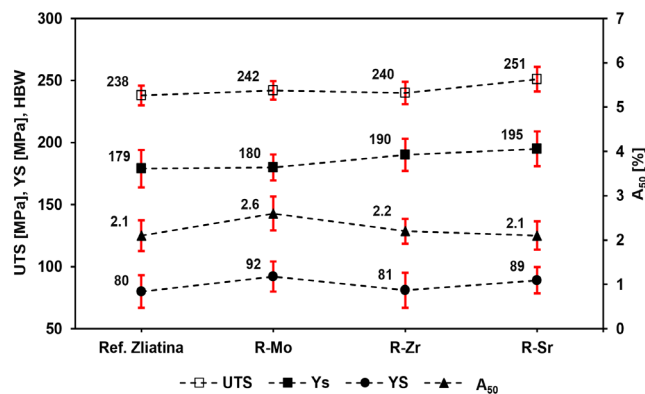
Fig. 3. Mechanical properties of experimental alloys after heat treatment T6

The mechanical properties of the experimental alloys increased under the influence of T6 heat treatment due to:
- spheroidization of eutectic Si to a more energetically favourable state of rounded grains,
- the presence of strengthening precipitates of Cu and Mg, which form strengthening precipitates of Al_2Cu and Mg_2Si due to the effect of T6.

3.2. Physical properties

The physical properties especially thermal conductivity of Al-Si-Cu-Mg alloys for high-stress automotive components is an important material characteristic that affects the functionality of high-stress automotive castings. Downsizing leads to an increase in the operating temperatures above 200 °C of the cylinder heads based on Al-Si-Cu-Mg. In general, the thermal stability of Al-Si-Cu-Mg alloys is limited by the thermal stability of strengthening precipitates θ-Al_2Cu and β-Mg_2Si. Strengthening precipitates are thermal stable up to the temperature 200 °C. Exceeding the temperature 200 °C leads to the coarsening and dissolution of strengthening precipitates, which causes to decrease in mechanical and physical properties of Al-Si-Cu-Mg alloys. Therefore, it is necessary to study the effect of alloying elements on the thermal conductivity of Al-Si-Cu-Mg alloys for high-stress automotive components.

The physical properties of the reference alloy, R-Mo, R-Sr and R-Zr in the cast state are processed in Fig. 4. The thermal and electrical conductivity of the experimental alloys with the addition of Zr, Mo and Sr in the as-cast state decreased significantly compared to the reference alloy. Compared to the reference alloy, a decrease in physical properties of 15 % on average was recorded for the alloy with the addition of Mo. The R-Sr alloy showed the smallest decrease in physical properties, on average 7 %, compared to the reference alloy. The largest decrease in physical properties was recorded by the R-Zr alloy. It is assumed that the significant decrease in the physical properties of the R-Zr alloy was caused by the morphology of intermetallic phases based on Zr. The Zr-rich phases tend to precipitate in the form of coarser needles with a split end or in the form of two crossed needles.

The physical properties of aluminum alloys are related to the scattering of electrons by the environment. The magnitude of electron scattering depends on the static imperfections present such as point defects, dislocations, impurities, or secondary phase particles. [20]

In general, any element added to an aluminum alloy acts as a barrier to the movement of free electrons [21,22]. The physical properties of experimental alloys with Mo, Zr and Sr decrease due to the action of Zr, Sr and Mo phases, which act as "impurities". Zr, Sr and Mo-rich phases block the electron transfer.
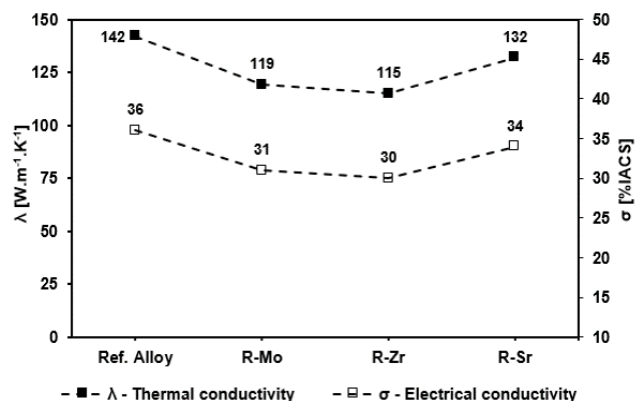
Fig. 4. Physical properties of experimental alloys in as-cast state [19]

The physical properties of the experimental alloys after the T6 heat treatment, depending on the added element, are processed into a graphical plot in Fig. 5. Due to the effect of T6 heat treatment, an increase in physical properties was recorded compared to the as-cast state. The thermal conductivity and electrical conductivity of the reference alloy increased by 30 %, and 31 %, respectively. The most significant increase in physical properties due to the effect of T6 was recorded by the experimental R-Zr alloy. Compared to the as-cast state, the thermal conductivity of the R-Zr alloy increased by 55 % and the electrical conductivity by 43 %. Due to the influence of T6, the R-Zr alloy achieved comparable values of physical properties with the reference alloy. Thermal conductivity of the R-Mo alloy increased by 36 % and the R-Sr alloy by 26 %, compared to the as-cast state.
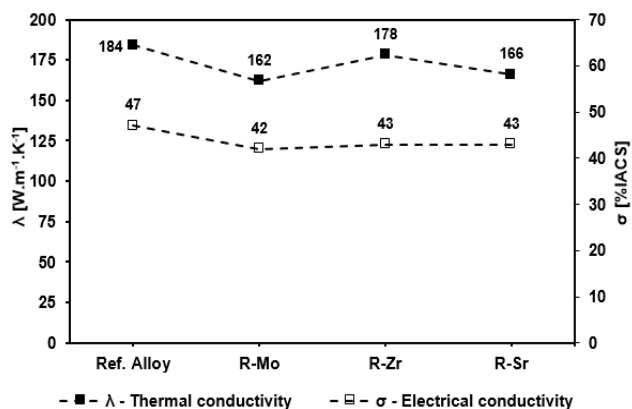
Fig. 5. Physical properties of experimental alloys after heat treatment T6

Based on the summarized results, it can be concluded that the increase in physical properties after T6 was due to a change in the morphology of eutectic Si. In the as-cast state, eutectic Si is excluded in the form of imperfectly round grains because AlSi5Cu2Mg alloy was supplied in a pre-modified state. Eutectic Si in the form of imperfectly round grains that block the passage of electrons through the medium (Fig. 6a). Due to the effect of T6 heat treatment, the morphology of eutectic Si changes to a more energetically favourable state of rounded grains (Fig. 6b) [22]. Eutectic Si segregated in the form of rounded grains ensures a more favourable transfer of free electrons, which leads to an increase in the physical properties of aluminum alloys [22,23].
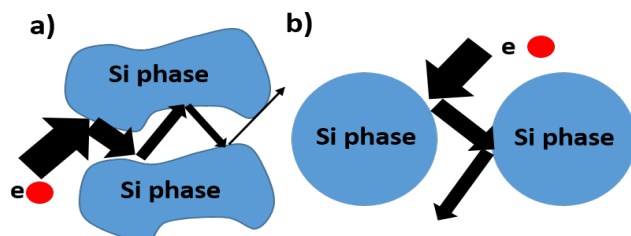
Fig. 6. Transfer of electrons: a) as-cast state; b) after heat treatment T6 [23]

3.2. Evaluation of microstructure, EDX analysis and fractographic evaluation

The microstructure of reference alloy in the as-cast state consists of α-phase, eutectic Si, and intermetallic phases based on Cu and Fe (Fig. 7a). In the plane of the metallographic cut eutectic Si can be observed in the form of imperfectly round grains. The morphology of the eutectic Si and the chemical composition of the reference alloy (Table 1) indicate that the AlSi5Cu2Mg alloy was supplied in a pre-modified state. Cu-rich intermetallic phases can be observed in the form of a ternary eutectic with a compact morphology. Due to the heat treatment T6, eutectic Si is spheroidized (Fig. 7b). Eutectic Si can be observed in the plane of the metallographic cut in the form of perfectly round grains.

The microstructure of the experimental alloy R-Zr in the as-cast-state consists of primary α-phase, eutectic Si, and intermetallic phases based on Cu and Fe (Fig. 7c). Intermetallic phases based on Cu were precipitated in the form of a ternary eutectic with a compact morphology. Fe-rich intermetallic phases were observed in the form of grey plates with cleaved terminations. The effect of T6 heat treatment is the spheroidization of the eutectic Si (Fig. 7d). Zr-rich intermetallic phases were not observed in the metallographic cut plane in the as-cast state and after heat treatment T6.

As in the previous case, the microstructure of the experimental alloy R-Sr consists of primary α-phase and eutectic Si (Fig. 7e). Local coarsening of eutectic Si or clustering of eutectic Si particles can also be observed in the metallographic cut plane due to excess Sr addition. Intermetallic phases based on Cu were observed in the form of ternary eutectic with a compact morphology. Due to the heat treatment T6, eutectic Si is spheroidized and Cu-rich intermetallic phases are observed in the form of isolated particles. (Fig. 7f).

As can be seen in Fig. 7g, the microstructure of the experimental alloy R-Mo in the as-cast state consists of primary α-phase and eutectic Si. The experimental Mo-I alloy was characterized by a local thickening of eutectic Si compared to Mo-R. Similar to previous case, local coarsening of eutectic Si can be observed. Intermetallic phases based on Cu can be observed in the metallographic cut plane. After heat treatment T6, eutectic Si can be observed in the form of perfectly round grains (Fig. 7h). Cu-rich phases are excluded in the form of isolated particles.

EDX analysis was performed on samples with the most favourable combination of mechanical properties. EDX analysis of experimental alloys with Zr addition demonstrated the presence of Zr-rich phases, which were identified as AlSiZr and Al$_3$Zr type phases. Intermetallic phases based on Zr were separated in the as-cast state (Fig. 8a) in the form of two crossed needles. An increased concentration of Cu and Fe was detected near the Zr-rich phases. Due to the effect of the T6 heat treatment, no changes in the morphology of the Zr-based intermetallic phases were observed compared to the as-cast state (Fig. 8b). This fact confirms the high thermal stability of the Zr-rich phases.

In the matrix of the experimental R-Sr alloy in the as-cast state, the presence of sharp-edged formations was detected - Fig. 8c. By EDX analysis, these particles were identified as polyhedral particles based on Al-Sr-Si. These particles were present in the plane of the metallographic cut due to the increased concentration of Sr in the melt. Derin states that the formation of particles based on Al-Sr-Si in Al-Si alloys occurs with the addition of 0.1 wt. % Sr [18]. As a result of the heat treatment, there was no change in the shape and size of the sharp-edged Sr-based formations (Fig. 8d).

On the basis of EDX analysis, intermetallic phases rich in Mo were detected in the R-Mo alloy in the cast state - Fig. 8e. An increased concentration of Fe was demonstrated near the Mo-rich phases. Intermetallic phases could be observed in the form of skeletal structures. By EDX analysis, the Mo-rich phases were identified as Al(FeMnMo)Si phases. Intermetallic phases β-Al5FeSi weren´t observed in the alloys with Mo addition. Due to the fact that Mo acts as a corrector of the ferrous phases, it is assumed that the crystallization of the β-Al5FeSi phase was

suppressed to form the more favourable Al(FeMnMo)Si-based intermetallic phases, which is in accordance with Morri's studies [9]. Due to the effect of T6 heat treatment, no significant change in the morphology of the intermetallic phases with increased Mo concentration was noted - Fig. 8f, which indicates the thermodynamic stability of these phases.

The matrix of experimetnal alloys consists of a solid solution of α in which eutectic Si crystals and intermetallic phases are precipitated. The solid solution α is characterized by the K12 lattice and very good plastic properties. Only very low plastic characteristics are achieved by the hard and brittle intermetallic phases. The shape and size of the eutectic Si and the amount of intermetallic phases affect the final appearance of the fracture surface.[12,24]

The relief of the fracture surface of the experimental alloys in the as-cast state does not differ significantly (Fig. 9a, c, e, g). The fracture surface of the experimental alloy in the as-cast state are identified by a transcrystalline ductile matrix fracture with pitting morphology and plastically reshaped α-phase ridges. The experimental alloys were supplied by the manufacturer in a pre-modified state. Due to the this fact eutectic Si on the fracture surfaces can be observed in the form of a skeleton with a common crystallization center. The cleavage facets on the fracture surface occurs due to the presence of the eutectic Si and intermetallic phases. The plastic and strength properties of intermetallic phases differ compared to those of the matrix. Depending on concentration, intermetallic phases can have different sizes and shapes [12,24].
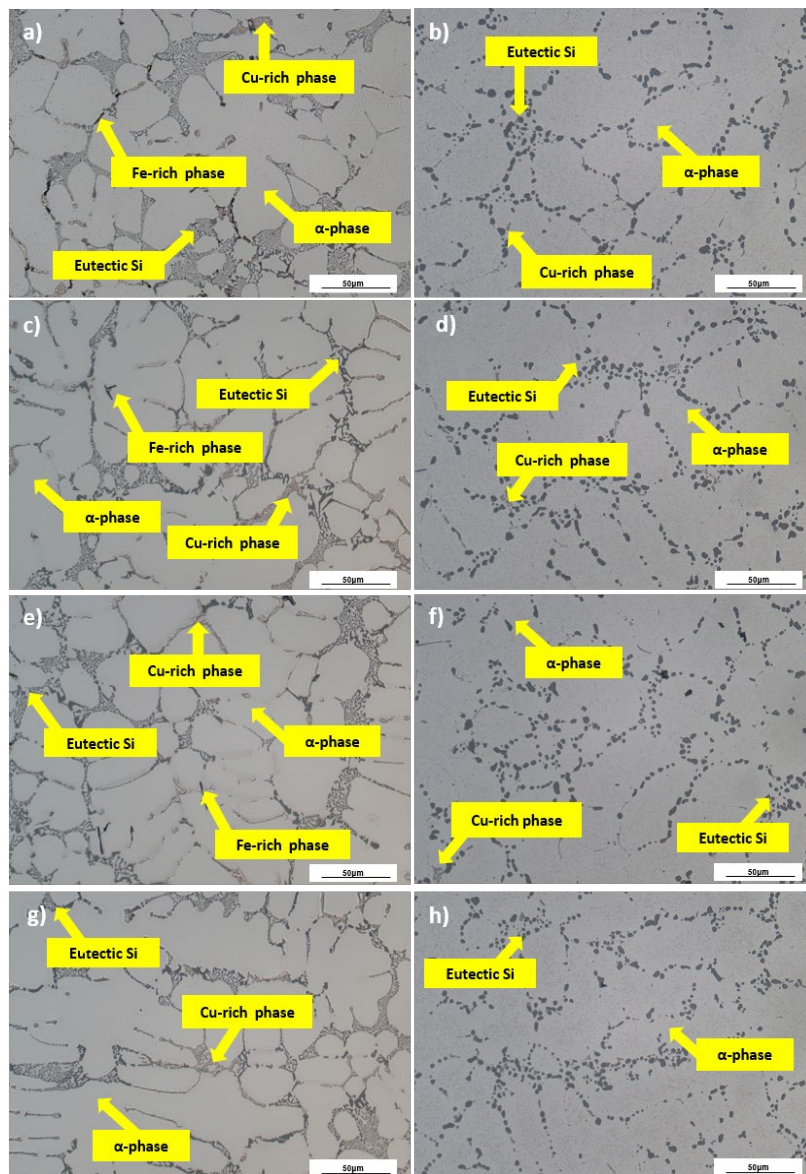
Fig. 7. Microstructural evaluation of experimental alloys in as-cast state and after heat treatment T6: a) Ref. alloy/AC; b) Ref. alloy/T6; c) R-Zr/AC; d) R-Zr/T6; e) R-Sr/AC; f) R-Sr/T6; g) R-Mo/AC; h) R-Mo/T6

Similar to previous case, the relief of the fracture surfaces of the experimental alloys after heat treatment T6 is characterized by a transcrystalline ductile matrix failure with pitted morphology and with plastically reshaped α-phase ridges (Fig. 9b, d, f, h). The result of the heat treatment T6 is the spheroidization of eutectic Si. Eutectic Si occur on the fracture surface in the form of isolated particles located at the bottom of the pits. The low plastic andstrenght properties of the intermetallic phases cause the presence of cleavage facets on the fracture surface.

6 Conclusions

The aim of the paper was to analyze the influence of selected alloying elements and heat treatment T6 on the selected properties and structure of the hypoeutectic AlSi5Cu2Mg alloy. Based on the obtained results, it can be concluded that:

- The addition of Zr, Sr in a given amount did not lead to a significant increase in the evaluated mechanical properties in the as-cast state and after heat treatment T6.
- The experimental alloy with Mo addition showed both in the cast state and after T6 heat treatment a positive increase in ductility above the ductility value achieved by the reference alloy. YS, UTS and HBW did not show a significant increase due to the addition of Mo.

- The physical properties of AlSi5Cu2Mg alloy decreased due to the addition of Mo, Zr and Sr. Alloying elements act as a barrier for the movement of electrons through the environment, which leads to a negative decrease in the physical properties of alloys with the addition of Zr, Sr and Mo.
- An increase in physical properties due to the spheroidization of eutectic Si was noted due to the effect of T6 heat treatment.
- The microstructure of experimental alloys in the as-cast state consist of α-phase, eutectic Si, and intermetallic phases based on Cu and Fe. As a result of increased Sr addition, a thickening of eutectic Si was observed, which may have had a negative impact on the mechanical properties of the AlSi5Cu2Mg alloy. Due to the heat treatment T6, eutectic Si is spheroidized. Mo, Sr and Zr-rich intermetallic phases were not observed in the metallographic cut plane in the as-cast state and after heat treatment T6.
- EDX analysis showed the presence of thermodynamically stable Al(FeMnMo)Si-based phases, which could lead to a positive increase in ductility. It is assumed that the ductility increased due to Mo acting as a corrector of the ferrous phases and suppressed the crystallization of the intermetallic phases β-Al$_5$FeSi.
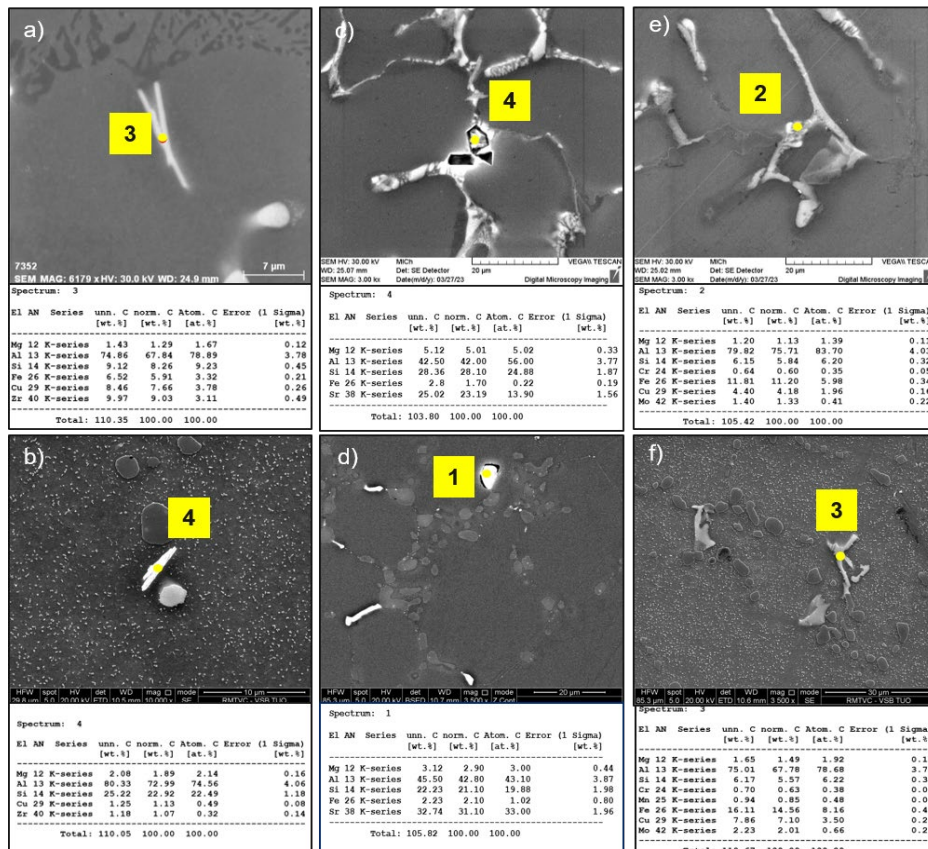
Fig. 8. EDX analysis of experimental alloys in as-cast state and after heat treatment T6: a) R-Zr/AC; b) R-Zr/T6; c) R-Sr/AC; d) R-Sr/T6; e) R-Mo/AC; f) R-Mo/T6
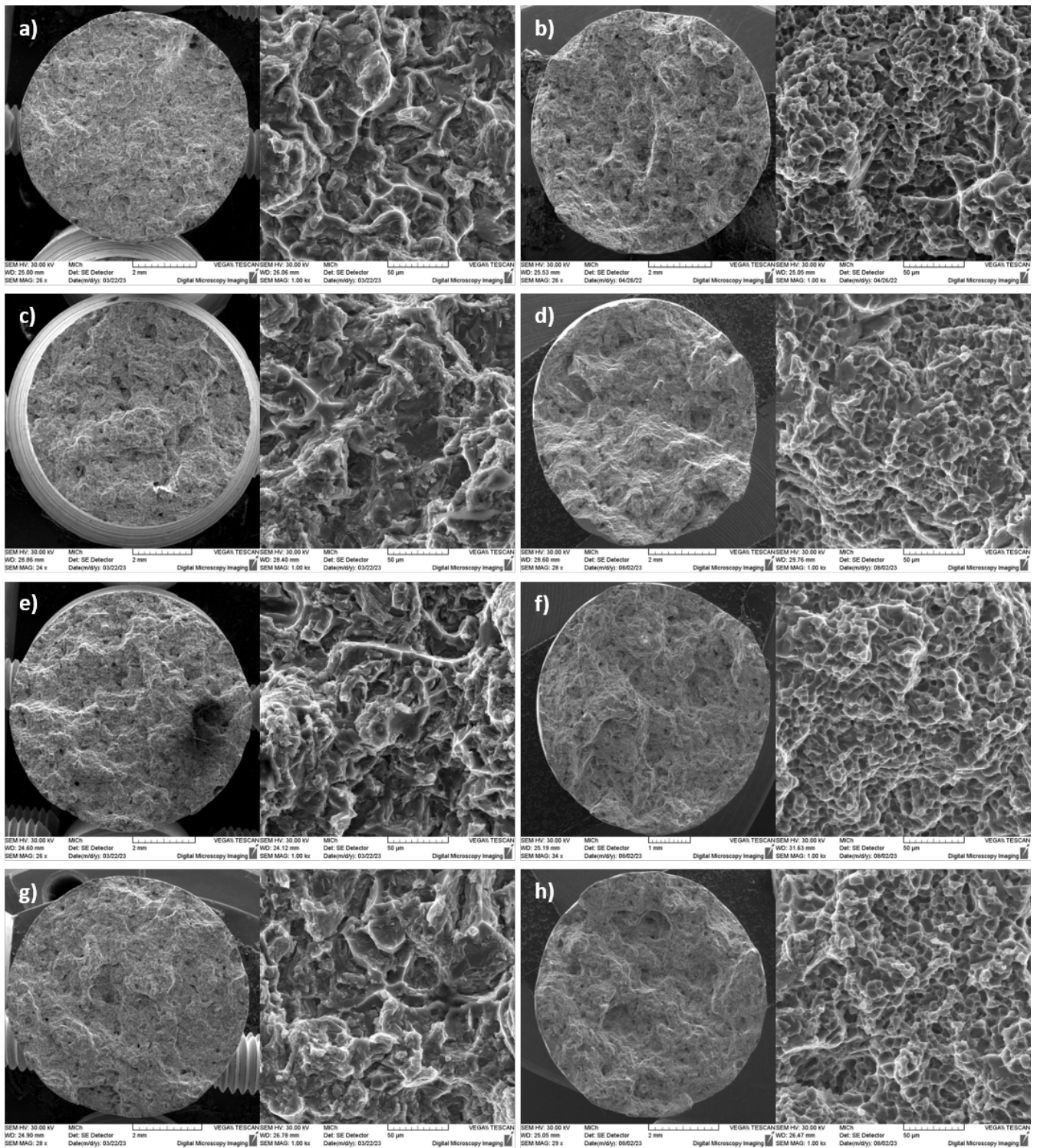
Fig. 9. Fractographic evaluation of experimental alloys in as-cast state and after heat treatment T6: a) R-Ref. alloy/AC; b) Ref. alloy/T6; c) R-Zr/AC; d) R-Zr/T6; e) R-Sr/AC; f) R-Sr/T6; g) R-Mo/AC; h) R-Mo/

- The presence of Zr-rich phases excluded in the form of typical crossed needles was proven in the R-Zr alloy. The morphology of intermetallic phases based on Zr was not affected by the T6 heat treatment. The presence of Zr-based phases could have negatively affect the resulting mechanical properties.
- The presence of sharp-edged particles with a high concentration of Sr was proven in the R-Sr alloy. These particles were identified by EDX analysis as polyhedral particles Al-Sr-Si.
- The relief of the fracture surface of the experimental alloys in the as-cast state and after heat treatment T6 does not differ significantly. The fracture surface of the experimental alloy in the as-cast state and after T6 re identified by a transcrystalline ductile matrix fracture with pitting morphology and plastically reshaped α-phase ridges. The presence of intermetallic phases causes the formation of cleavage facets on the fracture surface.

Based on the summarized results, it was shown that alloys with the addition of Zr and Sr in the above range do not show a significant increase in mechanical and physical properties, which could expand the field of application of AlSi5Cu2Mg alloy in the automotive industry at elevated operating conditions. From an application point of view, increased ductility is one of the key benefits in castings such as cylinder heads. Therefore, it is necessary to consider the potential benefit of Mo addition in achieving increased ductility, which is crucial for cylinder head castings.

Acknowledgements

References

[1] Yue, Z. & Liu, H. (2023). Advanced research on internal combustion engines and engine fuels. *Energies*. 16(16), 5940, 1-8. DOI: 10.3390/en16165940.

[2] Huang, Y., Surawski, N.C., Zhuang, Y., Zhou, J.L., Hong, G. (2021). Dual injections: an effectice and efficient technology to use renewablte fuels in spark ignition engines. *Renewable and Sustainable Energy Reviews*. 143, 110921. https://doi.org/10.1016/j.rser.2021.110921.

[3] Li, H. & Li, X. (2012). The present situation and the development trend of new materials used in automobile lightweight. *Applied Mechanics and Materials*. 189, 58-62. DOI: 10.4028/www.scientific.net/AMM.189.58.

[4] Czerwinski, F. (2021). Current trends in automotive lightweighting strategies and materials. *Materials*. 14(21), 6631, 1-27. DOI: 10.3390/ma14216631.

[5] Zhang, M., Wang, J., Wang. B., Xue, Ch. & Liu, X. (2022). Improving mechanical properties of Al-Si-Cu-Mg alloys by mircoalloying sc using thermodynamic calculations. *Calphad*. 76, 102394, 1-12. DOI:10.1016/j.calphad.2022.102394.

[6] Rakhmonov, J., Liu, K. & Chen, G. (2020). Effect of compositional variation on the thermal stability of θ´-Al2Cu precipitates and elevated temperature strengths in Al-Cu 206 alloys. *Journal of Materials Engineering and Performance*. 29, 7221-7230. DOI: 10.1007/s11665-020-05227-5.

[7] Czerwinski, F. (2020). Thermal stability of aluminum alloys. *Materials*. 13(15), 34441, 1-49. DOI: 10.3390/ma13153441.

[8] Rakhmonov, J., Timelli, G. & Bonollo, F. (2016). The effect of transition elements on high-temperature mechanical properties of al-si foundry alloys-a review. *Advanced Engineering Materials*. 18(7), 1096-1105. DOI:10.1002/adem.201500468.

[9] Morri, A., Ceschini, L., Messieri, S., Cerri, E. & Toschi, S. (2018). Mo addition to the A354 (Al-Si-Cu-Mg) casting alloy: effect on microstructure and mechanical properties at room and high temperature. *Metals*. 8(6), 393, 1-18. DOI: 10.3390/met8060393.

[10] Farkoosh, A.R., Chen, X.G. & Pekguleryuz, M. (2015). Interaction between molybdenum and manganese to form effective dispersoids in an Al-Si-Cu-Mg alloy and their influence on creep resistance. *Materials Science and Engineering A*. 627, 127-138. DOI: 10.1016/j.msea.2014.12.115.

[11] Gao, Ch., Zhang, L. & Zhang, B. (2021). Effect of transition metal elements on high-temperature properties of Al-Si-Cu-Mg alloys. *Metals*. 11(2), 357, 1-12. DOI: 10.3390/met11020357.

[12] Bolibruchová, D., Sýkorová, M., Brůna, M., Matejka, M. & Širanec, L. (2023). Effect of Zr addition on selected properties and microstructure of aluminum alloy AlSi5Cu2Mg. *International Journal of Metalcasting*. 17(4), 2596-2611. DOI: 10.1007/s40962-023-01048-z.

[13] Wang, F., Qui, D., Liu, Z., Taylor, J. A., Easton, M. A., Zhang, M. (2013). The grain refinement mechanism of cast aluminium by zirconium. *Acta Materialia*, 61(15), 5636-5645. DOI: 10.1016/j.actamat.2013.05.044.

[14] Sigli, C. (2004). Zirconium solubility in aluminum alloys. *Materials Science Forum*. 28, 1353-1358.

[15] Timpel, M., Wanderka, N., Schlesiger, R. & Yamamoto, T. (2012). The role of strontium in modifying aluminum-silicon alloys. *Acta Materialia*. 60(9), 3920-3928. DOI: 10.1016/j.actamat.2012.03.031.

[16] Sai Ganesh, M. R., Reghunath, N., Levin, M. J., Prasad, A., Doondi, S. & Shankar, K. V. (2021). Strontium in Al-Si-Cu-Mg alloy: a review. *Metals and Materials International*. DOI: 10.1007/s12540-021-01054-y.

[17] Ganesh, M., Reghunath, N., Levin, M., Prasad, A., Doondi, S., Shankar, K. (2021). Strontium in Al-Si-Mg Alloy: A Review. *Metals and Materials International*. DOI: 10.1007/s12540-021-01054-y.

[18] Derin, S., Birol, Y. (2016). Effect of strontium addition on microstructure and mechanical properties of AlSi7Mg0.3 alloy. *International Journal of Metalcasting*. 11(4), 1-8. DOI:10.1007/s40962-016-0117-4.

[19] Bolibruchová, D., Sýkorová, M. & Širanec, L. (2023). Influence of Sr, Zr and Mo on selected properties of

AlSi5Cu2Mg alloy. *Technológ*. 15(2), 52-57. DOI: 10.26552/tech.C.2023.2.8. (Slovak).

[20] Weng, W., Nagaumi, H., Sheng, X., Fan, W., Chen, X. & Wang, X. (2019). Influence of silicon phase particles on the thermal conductivity of Al-Si alloys. *The Minerals, Metals and Materials Society*. 193-198. DOI: 10.1007/978-3-030-05864-7_26.

[21] Zhang, A. & Li, Y. (2023). Thermal conductivity of aluminum alloys – a review. *Materials*. 16(8), 2972, 1-21. DOI: 10.3390/ma16082972.

[22] Li, K., Zhang, J., Chen, X., Yin, Y., He, Y., Zhou, Z. & Guan, R. (2020). Microstructure evolution of eutectic Si in Al-7Si binary alloy by heat treatment and its effect on enhancing thermal conductivity. *Journal of Materials Research and Technology*. 9(4), 8780-8786. DOI: 10.1016/j.jmrt.2020.06.021.

[23] Gan, J., Huang, Y., Wen, Ch. & Du, J. (2020). Effect of Sr modification on microstructure and thermal conductivity of hypoeutectic Al-Si alloys. *Transactions of Nonferrous Metals Society of China*. 30(11), 2879-2890. DOI: 10.1016/S1003-6326(20)65428-0.

[24] Tillová, E., Chalupová, M. (2009). *Structural analysis of Al-Si alloys*. Žilina: EDIS. ISBN 978-80-554-0088-4. (in Slovak).